

The Influence of Spatial and Temporal Distribution of Meteorology on Power System Operation

Fan Song¹, Yanling Wang^{1, *}, Guangling Gao², Xianghua Pan³,
Mingjun Zhang⁴, Likai Liang¹, and Zhijun Yin⁵

Abstract—Due to the spatial and temporal distribution of meteorological conditions along the transmission lines, the equivalent model with lumped parameters cannot accurately represent the line model with the actual parameters. In the paper, the nonuniform parameter model based on the dynamic thermal rating (DTR) technology of transmission lines is adopted to establish the power flow analysis model based on the conductor temperature. The algorithm presented in the paper is adopted to analyze the power flow of power networks with known load and meteorological parameters. And then cases with parameters of different seasons and spatial distribution in practical conditions are used to verify the feasibility of the algorithm. It is shown that the power flow analysis model established in this paper can realize the accurate analysis of the thermal load capacity of the transmission line in the power grid, which has great practical significance.

1. INTRODUCTION

With the rapid development of the national economy, the demand for electric energy is also constantly increasing. In 2017, the total electricity consumption reached 6307 TWh in Chinese society [1]. According to the assessment of future energy demand in China, electricity demand is expected to reach 7500 TWh in 2020 and 9730 TWh in 2030 [2]. In the context of increasing demand for electric energy and severely uneven distribution of new energy in China, it is particularly important to tap the load capability of existing transmission lines [3]. Thermal limitation of overhead transmission lines is a key factor limiting the load capacity of transmission components [4]. The application of dynamic thermal rating (DTR) technology can effectively improve the thermal load capacity of transmission lines [5]. However, the DTR technology is concerned with the thermal load capacity of the individual components. At the level of power grid operation, the current carrying capacity of transmission lines can be further tapped [6].

In [7], a kind of monitoring equipment of DTR system was proposed, including a load cell for monitoring the line tension, an ultrasonic anemometer for measuring the wind speed and direction, a solar radiation sensor, and an ambient temperature sensor. A method for indirect analysis of dynamic load capacity based on meteorological parameters was pointed in [8], which means simple and inexpensive system installation and post-maintenance. A method using modern meteorological numerical grid forecasting system was proposed for forecasting the thermal load capacity of transmission lines in [9]. This reduces the investment in hardware measurement equipment. However, the method did not effectively assess the accuracy of numerical forecast data. The importance of meteorological

Received 22 July 2018, Accepted 22 September 2018, Scheduled 4 October 2018

* Corresponding author: Yanling Wang (wangyanling@sdu.edu.cn).

¹ School of Mechanical, Electrical and Information Engineering, Shandong University, Weihai, Shandong 264209, China. ² State Grid of China Technology College, Jinan, Shandong 250000, China. ³ State Grid Shandong Electric Power Company, Jinan, Shandong 250000, China. ⁴ State Grid Jiamusi Power Supply Co. Ltd., Jiamusi, Heilongjiang 154000, China. ⁵ Shandong Inspur Software Company Limited, Jinan, Shandong 250000, China.

parameters to electric energy was introduced, and the temperature prediction played an important role in the operation of the power system [10]. The meteorological forecasting model applied to DTR was introduced in [11]. If the current atmospheric state is known, the future state can be obtained using the basic laws of standard physics. Canadian scholars proposed the basic concept of electric coordination in [12, 13]. This concept takes into account the physical laws of electrical and thermal coupling, as well as the discontinuity of the carrying capacity of transmission elements with the changing temperature. In [14, 15], the influence of temperature on the transmission line model was studied at the grid level. According to the change of ambient temperature gradient, the segmentation model of transmission line parameters related to ambient temperature was proposed to analyze the difference between the power flow system and the reference power flow system. But it is assumed that the conductor temperature is equal to the ambient temperature and the wind speed is zero. This is not consistent with the actual situation.

Although the DTR technology can effectively improve the current carrying capacity of overhead transmission lines, the cost of operation and maintenance of meteorological parameter monitoring equipment along the transmission lines is high. This paper will further improve the DTR technology. The conductor temperature is not only related to the complex meteorological conditions along the transmission lines and the physical parameters of conductors, but also related to the current carrying of the transmission lines. Hence, the conductor temperature is in a gradient distribution in space. In the traditional way of power flow analysis, the conductor parameters are usually taken as the nominal temperatures, and the line model generally adopts Π -type or T-type equivalent circuit model with lumped parameters. The parameters are essentially related to the conductor temperature, resulting in differences between the power flow analysis and the actual operating conditions. In view of the above problems, this paper analyzes the nonuniform parameter model based on conductor temperature and proposes line segmentation method according to the change of meteorological parameters along the transmission lines. Then, the actual transmission line parameters are obtained by the thermal balance equation. The power flow analysis model based on conductor temperature is proposed. Finally, the power flow analysis of the spatial and temporal distribution is analyzed.

The rest of this paper is organized as follows. The nonuniform parameter model based on the conductor temperature and the method of segment are proposed in Section 2. The power flow analysis based on the temperature of line is presented in Section 3. Case analysis based on a simple 5-bus power system is presented in Section 4. Section 5 concludes this paper.

2. OVERHEAD TRANSMISSION LINE MODEL BASED ON CONDUCTOR TEMPERATURE

2.1. Nonuniform Transmission Line Model Based on Conductor Temperature

The conductor resistance of the transmission line is related to its temperature, as shown in Eq. (1).

$$r(T) = r(T_0) \times [1 + \alpha(T - T_0)] \quad (1)$$

where T_0 is usually taken as 20°C, representing reference temperature; T is the given temperature; $r(T_0)$ is the resistance at reference temperature; $r(T)$ is the resistance at given temperature; α is the temperature coefficient of resistance (1/°C), which is determined by the physical material of the conductor.

Due to the change of line length caused by sag of the line, the conductor reactance of the transmission line is also related to the temperature, as shown in Eq. (2).

$$x_L(\omega, T) = x_L(\omega, T_0) \times [1 + \beta(T - T_0)] \quad (2)$$

where ω is the angular frequency in the power system; $x_L(\omega, T_0)$ is the line reactance at T_0 ; $x_L(\omega, T)$ is the line reactance at T ; β is temperature coefficient of reactance. Set $\alpha = \beta = 0.0039$ in the paper [16].

The Π -type or T-type equivalent circuit model with lumped parameters is widely used at present. In order to simplify the calculation, transmission line model with lumped parameters is mostly used to determine the status of the grid under no measurement conditions in power system state estimator and energy management systems, whose parameters are calculated at a certain temperature. The impedance and admittance of the transmission line conductor are not only related to the material

but also related to the conductor temperature. When the type of the line is selected, the parameters of the transmission line conductor during operation will be determined by its own temperature, and the conductor temperature is determined comprehensively by the ambient conditions and the current carrying capacity of the line. The meteorological parameters along the transmission lines are relatively complex. In order to accurately assess the operating status of the power grid, this paper analyzes the power flow by taking into account the differences in the conductor parameters, which are caused by the gradient of the conductor temperature.

The segmented transmission line model based on the conductor temperature is shown in Fig. 1.

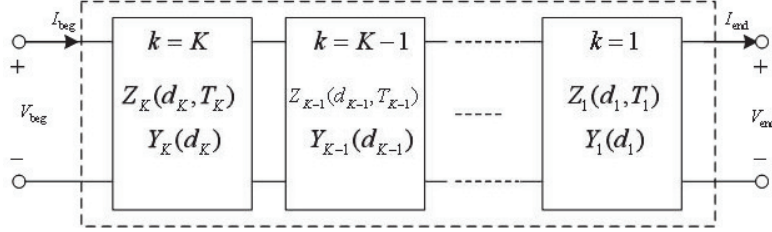


Figure 1. Segmentation parameter model of transmission line.

In Fig. 1, d_K is the length of segment K ; $Z_K(d_K, T_K)$ is the series impedance of segment K at temperature T_K ; $Y_K(d_K)$ is the parallel admittance of segment K ; V_{beg} and V_{end} are the voltages at the beginning and end of the branch respectively; I_{beg} and I_{end} are the currents at the beginning and end of the branch respectively.

2.2. Method of Transmission Line Segmentation

With the conductor temperature unknown, it is difficult for lines to segment according to the conductor temperature distribution. In this paper, the transmission line is segmented by key meteorological parameters, such as temperature or wind speed. Due to the randomness of wind speed, the transmission line is segmented according to ambient temperature. The parameters of each segment are obtained by the power flow analysis, and the line parameters under the given load and ambient parameters are obtained by the IEEE thermal balance equation [17], as shown in Eq. (3).

$$q_s + I^2 r(T) = q_r + q_c \tag{3}$$

where q_s is the absorption heat from solar radiation, mainly influenced by the sun radiation angle; I is the current; $r(T)$ is the conductor resistance; q_r is the radiation heat loss, mainly influenced by the conductor temperature and ambient temperature; q_c is the convection heat loss, mainly influenced by the conductor temperature, ambient temperature and wind speed.

The ambient temperature along the transmission lines can be obtained from numerical weather forecast. The temperature can be further spatially interpolated according to the spatial resolution of numerical weather forecast. Therefore, the fitting curve of the ambient temperature along the transmission lines can be obtained, as shown in Fig. 2. The beginning and end points of the branch are respectively x_{beg} and x_{end} .

In order to meet the needs of calculation accuracy and solution speed, the step length of the branch temperature segment is set in ΔT , then move the segmentation point from x_{beg} to x_{end} ; when the longitudinal temperature difference reaches ΔT , insert a segment point x_1 . Repeat above steps until the end of the branch, then calculate the ambient temperature of each segmented branch.

The ambient temperature and wind speed of each segment can be calculated by Eq. (4).

$$\left. \begin{aligned} T_{\text{avg}} &= (T_{\text{beg}} + T_{\text{end}})/2 \\ V_{\text{avg}} &= (V_{\text{beg}} + V_{\text{end}})/2 \end{aligned} \right\} \tag{4}$$

where T_{beg} and T_{end} are the ambient temperatures at the beginning and end of the branch, respectively; T_{avg} is the ambient temperature of each segment; V_{beg} and V_{end} are the wind speeds at the beginning and end of the branch, respectively.

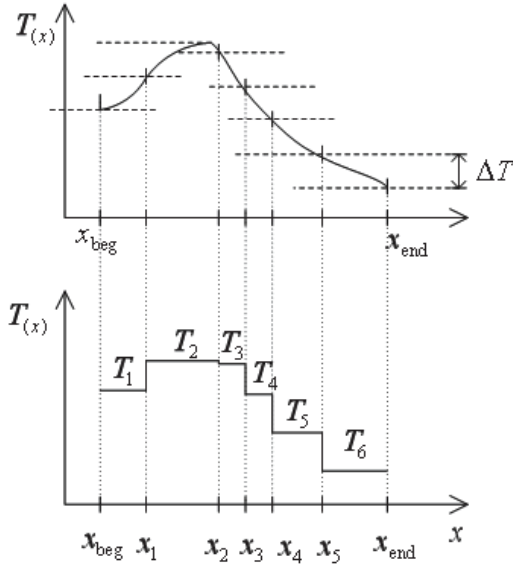


Figure 2. Segmentation method and ambient temperature curve along the transmission lines.

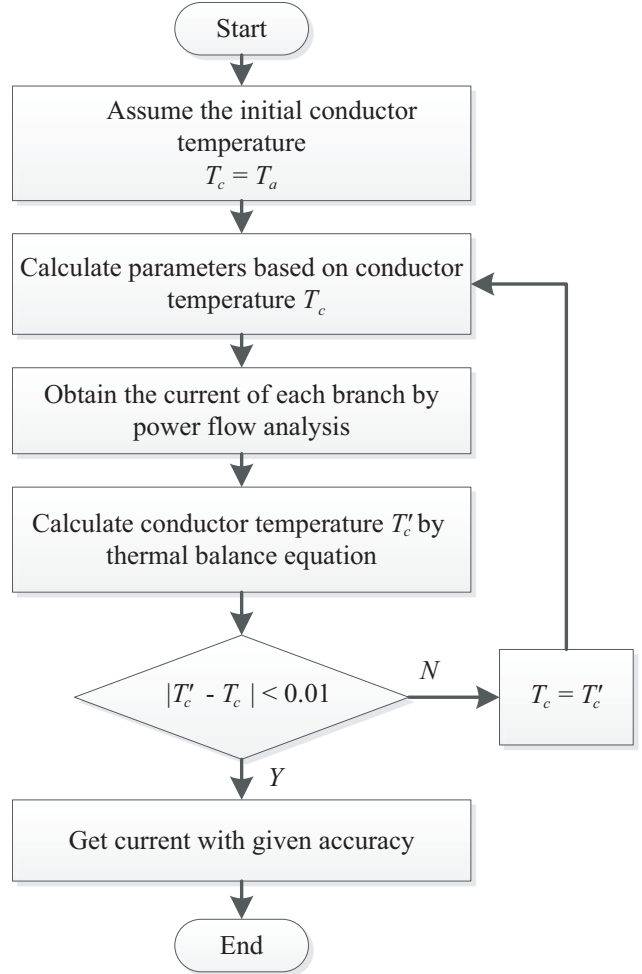


Figure 3. Power flow analysis based on conductor temperature.

3. POWER FLOW ANALYSIS BASED ON CONDUCTOR TEMPERATURE

The conditions of the algorithm proposed in this section are that the grid load is constant, and the meteorological parameters are known. It is assumed that the impedance and admittance of the transmission lines are constant in the power flow analysis used in the past. In practice, the current carrying value of each transmission line is different. Due to the spatial distribution of the power grid, the meteorological parameters along the various transmission lines are different, and the actual conductor temperatures are also different according to the IEEE thermal balance equation. The method of power flow analysis proposed in this section takes above factors into account, and power flow analysis algorithm based on the conductor temperature is proposed. The specific algorithm flow is shown in Fig. 3.

The specific steps of the power flow analysis based on the actual conductor temperature are as follows:

(1) It is assumed that the conductor temperature T_c is the ambient temperature T_a . The impedance and admittance of the transmission line conductor at this time are calculated, the power flow of the power grid is analyzed, and the current carrying value of each branch is obtained at this time;

(2) Based on the IEEE thermal balance equation, the actual conductor temperature T_c' is calculated according to the meteorological parameters and the current carrying value of transmission lines obtained by the first step;

(3) Determine whether $|T_c' - T_c|$ is less than the specified accuracy. If not, the conductor temperature is set to $T_c = T_c'$, the conductor parameters at the temperature T_c are calculated. Repeat the first step and the second step;

(4) If $|T_c' - T_c|$ is less than the specified accuracy, the conductor temperature is the actual operating temperature, and the power flow results obtained at this time are more accurate with given accuracy.

In this section, the power flow analysis algorithm based on the conductor temperature is generally iterated three times in the actual calculation to meet the accuracy requirements. Considering the conductor temperature under actual meteorological conditions and loads in the power grid, the result of the power flow analysis using the calculated conductor parameters is closer to the actual operation state of the power grid. This has great application value.

4. CASE STUDY

In order to reveal the significance of the power flow model based on conductor temperature, a simple 5-bus system for power flow analysis in different environments is presented in this paper. The type of the line in this case is LGJ-400/50 whose diameter is 27.63 mm. The cross-sectional area of aluminum line is 399.7 mm^2 , and its resistance is $0.07232 \Omega/\text{km}$ at 20°C , and the temperature coefficient of resistance is $0.0039 \Omega/^\circ\text{C}$.

The lengths of the branches 2-1, 3-1, and 2-3 in the system are respectively 120 km, 120 km, and 200 km. In the base case, the conductor temperature of each branch is 20°C without considering meteorological parameters. The reference voltage of the grid is 220 kV and the reference capacity is 100 MVA. The grid structure and per-unit value of each component parameters are shown in Fig. 4.

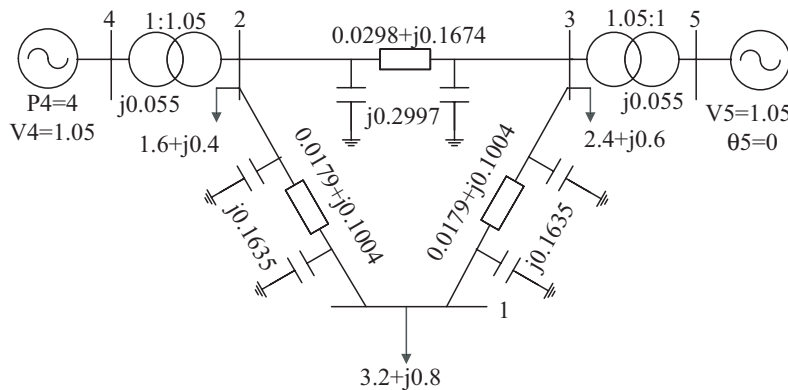


Figure 4. Grid structure and per-unit value of parameters.

In addition to the base case, the ambient conditions include extreme weather conditions and the spatial distribution of meteorological conditions. The power flow model based on the conductor temperature is used to analyze the running state of the grid system in different cases.

Case 1, case 2, case 3, and case 4 are set up respectively. Case 1 and case 2 are compared with the base case in the temporal distribution of power flow; case 3 and case 4 are compared with the base case in the spatial distribution of power flow.

4.1. Base Power Flow Analysis

The conductor temperature in the grid system is assumed to be 20°C without considering the meteorological conditions along the transmission lines (20°C is a common reference situation in grid analysis) in the base case. Using the power flow model based on the conductor temperature, the conductor temperature, conductor parameters, and current values of the branches 2-1, 3-1 and 2-3 at this time are obtained, as shown in Table 1.

Table 1. Related parameters in base case.

Branch	Conductor temperature (°C)	r (p.u.)	x_L (p.u.)	I (A)
2-1	20	0.0179	0.1004	519.66
3-1	20	0.0179	0.1004	359.94
2-3	20	0.0298	0.1674	114.94

4.2. Power Flow Analysis in Seasonal Distribution of Meteorological Conditions

4.2.1. Case 1

It is assumed that the ambient temperature is -40°C , and the wind speed is 22 m/s, such as strong wind and extremely cold areas in winter in northern China. According to the ambient temperature and wind speed along the lines, the conductor temperature, conductor parameters, and current values of the branches 2-1, 3-1 and 2-3 at this time are obtained using the power flow model based on the actual conductor temperature, as shown in Table 2, where “*Error*” represents the current difference compared with the base case.

Table 2. Related parameters in case 1.

Branch	Ambient temperature (°C)	Wind speed (m/s)	Conductor temperature (°C)	r (p.u.)	x_L (p.u.)	I (A)	<i>Error</i> (%)
2-1	-40	22	-36.713	0.0139	0.0782	510.23	-1.81
3-1	-40	22	-37.413	0.0139	0.0779	345.88	-3.9
2-3	-40	22	-37.943	0.0231	0.1296	115.28	0.3

4.2.2. Case 2

It is assumed that the ambient temperature is 40°C , and the wind speed is 0.5 m/s, such as high temperature and less wind areas in summer in China. According to the ambient temperature and wind speed along the lines, the conductor temperature, conductor parameters, and current values of the branches 2-1, 3-1 and 2-3 at this time are obtained using the power flow model based on the actual conductor temperature, as shown in Table 3.

Table 3. Related parameters in case 2.

Branch	Ambient temperature (°C)	Wind speed (m/s)	Conductor temperature (°C)	r (p.u.)	x_L (p.u.)	I (A)	<i>Error</i> (%)
2-1	40	0.5	65.913	0.0211	0.1184	524.21	0.88
3-1	40	0.5	59.585	0.0207	0.1159	376.89	4.71
2-3	40	0.5	54.067	0.0338	0.1896	118.21	2.84

The comparisons of the active power flow and active power losses of case 1 and case 2 with that of the base case are shown in Table 4 and Table 5, respectively. In Table 4, 2-1(2) indicates bus 2 at the beginning of branch 2-1. Others are the same as above.

The maximum difference of the conductor temperature between case 1 and case 2 is 102.6°C , which is greater than 80°C of the difference from the ambient temperature. The conductor temperature is about -37°C in case 1, which is far below the boundary operating temperature of 70°C , indicating that the thermal load potential of the transmission lines under this ambient condition (gale area in winter)

Table 4. Comparisons of active power flow of case 1, case 2 and base case.

Branch	Base case (MW)	Case 1 (MW)	<i>Error</i> (%)	Case 2 (MW)	<i>Error</i> (%)
2-1(2)	198.34	197.85	-0.25	197.13	-0.61
2-1(1)	-191.15	-192.48	0.7	-188.48	-1.4
3-1(3)	132.38	130.04	-1.77	136	2.74
3-1(1)	-128.85	-127.52	-1.03	-131.52	2.07
2-3(2)	41.66	42.15	1.18	42.87	2.9
2-3(3)	-41.18	-41.77	1.43	-42.29	2.7

Table 5. Comparisons of the active power losses of case 1, case 2 and base case.

Case	Base case (MW)	Case 1 (MW)	<i>Error</i> (%)	Case 2 (MW)	<i>Error</i> (%)
Active power loss	11.2	8.27	-26.16	13.72	22.5

is very large. The conductor temperature reaches 65.9°C in case 2, closing to the boundary operating temperature of 70°C , indicating that the thermal load capacity of the transmission lines under this ambient condition (high temperature and less wind area in summer) is close to the limit.

The conductor temperature is relatively low, and the impedance is small in case 1, so that the active power losses of the grid is 26.16% lower than that of the base case. However, the conductor temperature is relatively high and the impedance is large in case 2, so that the active power losses of the power grid is 22.5% more than that of the base case. The distributions of active power flow are relatively insignificant in case 1, case 2 and base case.

4.3. Power Flow Analysis in Spatial Distribution of Meteorological Conditions

It is assumed that the ambient temperature of branch 2-1 is 20°C , and the wind speed is 0.5 m/s. The ambient temperature of bus 3 is 0°C , and the wind speed is 20 m/s. The ambient temperature and wind speed along branch 2-3 and branch 1-3 are linearly distributed (above environmental conditions occur in extreme climatic conditions such as cold waves in the area). The spatial distribution of conductor temperature caused by the difference of the meteorological parameters along the transmission lines and its influence on the running state of power grid are studied.

4.3.1. Case 3

The ambient temperature and wind speed in case 3 are taken as the average of the beginning and end of each branch. According to the ambient temperature and wind speed along the lines, the conductor temperature, conductor parameters, and current values of branches at this time are obtained using the power flow model based on the actual conductor temperature, as shown in Table 6.

Table 6. Related parameters in case 3.

Branch	Ambient temperature ($^{\circ}\text{C}$)	Wind speed (m/s)	Conductor temperature ($^{\circ}\text{C}$)	r (p.u.)	x_L (p.u.)	I (A)	<i>Error</i> (%)
2-1	20	0.5	45.944	0.0197	0.1106	503.18	-3.17
3-1	10	10.25	14.52	0.0175	0.0983	381.83	6.08
2-3	10	10.25	13.335	0.0290	0.1630	129.70	12.84

4.3.2. Case 4

In case 4, branch 2-3 and branch 1-3 are segmented by ambient temperature. Set the step length is 4°C. Branch 2-3 and branch 1-3 are divided into five segments respectively. The ambient temperature and wind speed of each segment are the mean values of ambient temperatures and wind speeds at the beginning and the end of the branch. The number of each bus and the structure of the power grid are shown in Fig. 5.

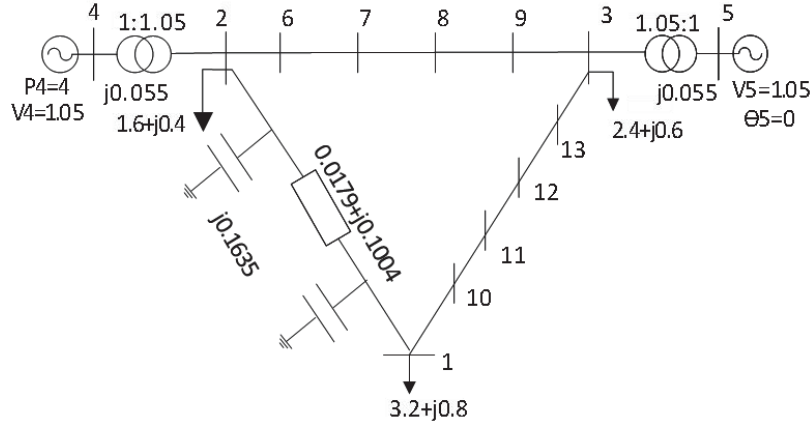


Figure 5. Structure of power grid after segmentation.

According to the ambient temperature and wind speed along the lines, the conductor temperature, conductor parameters, and current values of branches at this time are obtained using the power flow model based on the actual conductor temperature, as shown in Table 7. The comparisons of the active power flow of case 3 and case 4 with that of the base case are shown in Table 8.

Table 7. Related parameters in case 4.

Branch	Ambient temperature (°C)	Wind speed (m/s)	Conductor temperature (°C)	r (p.u.)	x_L (p.u.)	I (A)	Error (%)
2-1	20	0.5	45.078	0.0197	0.1102	502.66	-3.27
1-10	18	2.55	28.069	0.0037	0.0205	397.16	10.34
10-11	14	6.65	19.931	0.0036	0.0199	394.27	9.54
11-12	10	10.75	14.476	0.0035	0.0196	391.27	8.70
12-13	6	14.85	9.678	0.0034	0.0192	388.18	7.85
13-3	2	18.95	5.157	0.0034	0.0189	385.02	6.97
2-6	18	2.55	25.182	0.0061	0.0342	129.80	12.93
6-7	14	6.65	18.249	0.0059	0.0333	125.05	8.80
7-8	10	10.75	13.228	0.0058	0.0326	122.07	6.20
8-9	6	14.85	8.675	0.0057	0.0320	121.00	5.27
9-3	2	18.95	4.319	0.0056	0.0314	121.91	6.09

In case 3 and case 4, the highest conductor temperatures are similar, which are 45.94°C and 45.08°C, respectively. The conductor temperatures of the middle section of branch 3-1 and branch 2-3 in case 4 are similar to that of in case 3. The conductor temperatures are 14.52°C and 13.34°C in case 3, while they are 14.48°C and 13.23°C in case 4. It is indicated that the two models have little effect on the conductor temperature. The advantage of case 4 is that it can more accurately reflect the actual distributions of the conductor temperatures of branch 3-1 and branch 2-3.

Table 8. Comparisons of the active power flow of case 3, case 4 and base case.

Branch	Base case (MW)	Case 3 (MW)	<i>Error (%)</i>	Case 4 (MW)	<i>Error (%)</i>
2-1(2)	198.34	191.7	-3.35	191.59	-3.4
2-1(1)	-191.15	-184.26	-3.6	-184.19	-3.64
3-1(3)	132.38	139.61	5.46	139.67	5.51
3-1(1)	-128.85	-135.74	5.35	-135.81	5.4
2-3(2)	41.66	48.3	15.94	48.41	16.2
2-3(3)	-41.18	-47.68	15.78	-47.77	16

Case 3 and case 4 are significantly different from the base case in the current, with a maximum of 12.93%. Likewise, case 4 can more accurately reflect the current distributions of branch 3-1 and branch 2-3. For example, the maximum current of branch 3-1 is 397.16 A and the lowest is 385.02 A. The inconsistency of line parameters in space caused by the different conductor temperature makes the active power flow significantly different from the base case, which is up to 16.2%. Further comparisons of the currents, active power flow and active power losses in case 1, case 2, case 3, case 4 and base case are shown in Table 9. The differences of the active power losses between case 3, case 4 and the base case are smaller than that of case 1, case 2 and the base case, because there is a small difference between the conductor temperature and the reference temperature.

Table 9. The current, active power flow and active power loss in five cases.

Case	Current			Active power flow						Active power loss
	2-1	3-1	2-3	2-1(2)	2-1(1)	3-1(3)	3-1(1)	2-3(2)	2-3(3)	
Base case	519.66	359.94	114.94	198.34	-191.15	132.38	-128.85	41.66	-41.18	11.2
Case 1	510.23	345.88	115.28	197.85	-192.48	130.04	-127.52	42.15	-41.77	8.27
<i>Error (%)</i>	-1.81	-3.9	0.3	-0.25	0.7	-1.77	-1.03	1.18	1.43	-26.16
Case 2	524.21	376.89	118.21	197.13	-188.5	136	-131.52	42.87	-42.29	13.72
<i>Error (%)</i>	0.88	4.71	2.84	-0.61	-1.4	2.74	2.07	2.9	2.7	22.5
Case 3	503.18	381.83	129.70	191.7	-184.26	139.61	-135.74	48.3	-47.68	11.94
<i>Error (%)</i>	-3.17	6.08	12.84	-3.35	-3.6	5.46	5.35	15.94	15.78	6.61
Case 4	502.66	397.16	129.8	191.59	-184.19	139.67	-135.81	48.41	-47.77	11.9
<i>Error (%)</i>	-3.27	10.34	12.93	-3.4	-3.64	5.51	5.4	16.2	16	6.25

5. CONCLUSIONS

Due to different conductor temperatures caused by the complex ambient conditions and different current values, the segment model of the transmission line based on the conductor temperature is adopted. On the basis of this, due to the invariance of parameters in the lumped parameter power flow model, a power flow model based on the actual conductor temperature is proposed according to the IEEE thermal balance equation. Based on the above models, case 1 and case 2 take into account the seasonal variations of the meteorological conditions. For an ideal uniform meteorological parameters model, without considering the spatial difference, the active power loss will decrease with the decrease of ambient temperature and the increase of wind speed for the system with certain structure and parameters. For active power flow, it depends not only on meteorological parameters, but also on the structure and parameters of the system. Case 3 and case 4 consider the nonuniform spatial distribution of meteorological conditions. The results show that the active power flow and current distribution can be determined more precisely using the segment model, and then the power flow can be more effectively evaluated.

ACKNOWLEDGMENT

This paper is supported by the National Natural Science Foundation of China (51407111, 51407106, 51641702), the Science and Technology Development Project of Shandong Province, China (ZR2015ZX045), and the Science and Technology Development Project of Weihai City (2014DXGJ23).

REFERENCES

1. Jiang, X. L., "Analysis of the situation of power development and reform in China (2018)," *China Electrical Equipment Industry*, No. 5, 15–29, 2018.
2. Yuan, J. H., Q. Lei, and M. P. Xiong, "The prospective of coal power in China: Will it reach a plateau in the coming decade?," *Energy Policy*, Vol. 98, 495–504, 2016.
3. Gao, H., J. C. Liu, and J. Y. Liu, "Analysis and research of transmission corridor planning under the global energy network," *Sichuan Electric Power Technology*, Vol. 40, No. 3, 15–20, 2017.
4. Wang, M. X., X. S. Han, and H. B. Sun, "Analysis of enhancing power grid's capacity to absorb intermittent power generation based on electric heating coordination theory," *Sichuan Electric Power Technology*, Vol. 33, No. 9, 7–12, 2013.
5. Zhan, J., C. Y. Chung, and E. Demeter, "Time series modeling for dynamic thermal rating of overhead lines," *IEEE Transactions on Power Systems*, Vol. 32, No. 3, 2172–2182, 2017.
6. Ying, Z. F., Y. S. Chen, and K. Feng, "New DTR estimation method without measured solar and wind data," *Journal of Electrical Engineering and Technology*, Vol. 12, No. 2, 576–585, 2017.
7. Ringelband, T., P. Schafer, and A. Moser, "Probabilistic ampacity forecasting for overhead lines using weather forecast ensembles," *Electrical Engineering*, Vol. 95, No. 2, 99–107, 2013.
8. Babs, A., "Weather-based and conductor state measurement methods applied for dynamic line rating forecasting," *Proceedings of the International Conference on Advanced Power System Automation and Protection*, 2011.
9. Zhou, H. S., Z. Chen, and J. Zhang, "Application of meteorological numerical forecast technology for improving transmission line capability," *Power System Technology*, Vol. 40, No. 7, 2175–2180, 2016.
10. Troccoli, A., L. Dubus, and S. E. Haupt, *Weather Matters for Energy*, Springer, New York, 2014.
11. Michiorri, A., H. M. Nguyen, and S. Alessandrini, "Forecasting for dynamic line rating," *Renewable and Sustainable Energy Reviews*, Vol. 52, 1713–1730, 2015.
12. Banakar, H., N. Alguacil, and F. D. Galiana, "Electrothermal coordination Part I: Theory and implementation schemes," *IEEE Transactions on Power Systems*, Vol. 20, No. 2, 798–805, 2005.
13. Alguacil, N., M. H. Banakar, and F. D. Galiana, "Electrothermal coordination Part II: Case studies," *IEEE Transactions on Power Systems*, Vol. 20, No. 4, 1738–1745, 2005.
14. Cecchi, V., M. Knudson, and K. Miu, "System impacts of temperature-dependent transmission line models," *IEEE Transactions on Power Delivery*, Vol. 28, No. 4, 2300–2308, 2013.
15. Cecchi, V., A. S. Leger, and K. Miu, "Incorporating temperature variations into transmission-line models," *IEEE Transactions on Power Delivery*, Vol. 26, No. 4, 2189–2196, 2011.
16. Aaron, S. L. and N. Chika, "OTA-based transmission line model with variable parameters for analog power flow computation," *International Journal of Circuit Theory and Applications*, Vol. 38, 199–220, 2008.
17. Teh, J. and I. Cotton, "Critical span identification model for dynamic thermal rating system placement," *IET Generation, Transmission and Distribution*, Vol. 9, No. 16, 2644–2652, 2015.